

# Anthropogenic radionuclides in the water column and a sediment core from the Alboran Sea: application to radiometric dating and reconstruction of historical water column radionuclide concentrations

A. Laissaoui · M. Benmansour · N. Ziad · M. Ibn Majah · J. M. Abril · S. Mulsow

**Abstract** Global fallout is the main source of anthropogenic radionuclides in the Mediterranean Sea. This work presents  $^{137}\text{Cs}$ ,  $^{239+240}\text{Pu}$  and  $^{241}\text{Am}$  concentrations in the water column in the southwest Alboran Sea, which was sampled in December 1999. A sediment core was taken at 800 m depth in the area ( $35^{\circ}47' \text{ N}$ ,  $04^{\circ}48' \text{ W}$ ).  $^{210}\text{Pb}$ ,  $^{226}\text{Ra}$ ,  $^{137}\text{Cs}$  and  $^{239+240}\text{Pu}$  specific activities were measured at multiple depths in the core for dating purposes.  $^{137}\text{Cs}$  and  $^{239+240}\text{Pu}$  profiles did not show defined peaks that could be used as time markers, and they extended up to depths for which the  $^{210}\text{Pb}$ -based constant rate of supply (CRS) dating model provided inconsistent dates. These profiles can be useful to test dating models, understood as particular solutions of a general advection–diffusion problem, if the time series of radionuclide inputs into the sediment is provided. Thus, historical records of depth-averaged  $^{137}\text{Cs}$  and  $^{239+240}\text{Pu}$  concentrations in water, and their corresponding fluxes into the sediment, were

reconstructed. A simple water-column model was used for this purpose, involving atmospheric fallout, measured distribution coefficient ( $k_d$ ) values, and a first-estimate of sedimentation rates. A dating model of constant mixing with constant sedimentation rate was applied successfully to three independent records (unsupported  $^{210}\text{Pb}$ ,  $^{137}\text{Cs}$  and  $^{239+240}\text{Pu}$ ), and provided the objective determination of mixing parameters and mass sedimentation rate. These results provide some insight into the fate of atmospheric inputs to this marine environment and, particularly, into the contribution from the Chernobyl accident.

**Keywords** Alboran Sea · Sedimentation rate · Anthropogenic radionuclides · Radiometric dating · Constant mixing · Dating model

## Introduction

The main sources of anthropogenic radionuclides in the Mediterranean Sea are global fallout from atmospheric nuclear weapon tests carried out mainly in the 1950s and the early 1960s, and the Chernobyl accident which occurred in 1986 (e.g. Delfanti et al. 1995; Molero et al. 1995; Papucci et al. 1996; León Vintro et al. 1999; Lee et al. 2003). The global inputs of  $^{137}\text{Cs}$  and  $^{239+240}\text{Pu}$  to the Mediterranean Sea up to 1986 are estimated to be 12 PBq and 0.19 PBq, respectively (Holm et al. 1988; UNEP 1992). The Chernobyl

---

A. Laissaoui (✉) · M. Benmansour · N. Ziad ·  
M. Ibn Majah  
Centre National de l'Énergie des Sciences et des  
Techniques Nucléaires, B.P. 1382, 10001 Rabat, Morocco  
e-mail: laissaoui@cnesten.org.ma

J. M. Abril  
Dpto. Física Aplicada I, EUITA, University of Seville,  
Carretera de Utrera km 1, 41013 Seville, Spain

S. Mulsow  
Instituto Geociencias, Universidad Austral de Chile,  
Casilla 567, Valdivia, Chile

accident significantly increased the total input of  $^{137}\text{Cs}$  into the environment of the Mediterranean Sea. Pappuci et al. (1996) estimated that about 2.5 PBq of  $^{137}\text{Cs}$  were deposited after the accident, mainly in the eastern and northern parts of the Mediterranean basin. However, the distribution of anthropogenic radionuclides in the southwest Mediterranean has not been well established. Therefore one of the objectives of this work has been to study levels of  $^{137}\text{Cs}$ ,  $^{239+240}\text{Pu}$  and  $^{241}\text{Am}$  in the water column (up to 900 m depth) in the southwest Alboran Sea. A sediment core was sampled at 800 m depth in the area ( $35^{\circ}47' \text{ N}$ ,  $04^{\circ}48' \text{ W}$ ). Radiometric dating of this core, i.e. measurement of unsupported  $^{210}\text{Pb}$ ,  $^{137}\text{Cs}$  and  $^{239+240}\text{Pu}$  profiles, provides insight into the fate of atmospheric inputs in this marine environment.

Marine sediments play an important role as a final reservoir for radioactive pollutants (Laissaoui and Abril 1999; Laissaoui et al. 1998).  $^{210}\text{Pb}$ , a member of the  $^{238}\text{U}$  natural decay series, is produced in the atmosphere by radioactive decay of  $^{222}\text{Rn}$  emanating from the earth's surface, and has been used extensively to study accumulation and mixing processes in coastal marine sediment (Abril et al. 1992; Sanchez-Cabeza and Molero 2000). Aerosol  $^{210}\text{Pb}$  falling directly into surface water is scavenged and deposited in sediments with any  $^{226}\text{Ra}$ -supported  $^{210}\text{Pb}$  of lithogenic origin. Preservation of  $^{210}\text{Pb}$  activity in excess of any  $^{226}\text{Ra}$ -supported  $^{210}\text{Pb}$  in accumulating sediments provides a useful chronological tool for studying recent sedimentation processes over time-scales of about 100–150 years. Abril (2003a) reviewed radiometric dating models using a new theoretical treatment of compaction and the advective-diffusive processes in sediments. Different dating models can be understood as particular solutions of such a general advection–diffusion problem.  $^{210}\text{Pb}$ -based models are the simplest since steady-state can be reasonably assumed. The most popular  $^{210}\text{Pb}$ -based models are the CRS (Constant Rate of Supply) model, from Appleby and Oldfield (1978), and the CIC-CSR (Constant Initial Concentration with Constant Sedimentation Rate) model (see Robbins 1978). Other models are the CMZ (Complete Mixing Zone) and IMZ (Incomplete Mixing Zone) models, from Robbins and Edginton (1975), and Abril et al. (1992), respectively, or the CM-CSR (Constant Mixing with Constant Sedimentation Rate) model used by Smith et al. (1986). These models

have become the methods of choice for determining sediment age–depth relations. However, the  $^{210}\text{Pb}$ -based geochronology should be validated using at least one independent tracer that provides an unambiguous, independent time-marker, such as fallout  $^{137}\text{Cs}$  (Smith 2001). Most recently, Abril (2003b, 2004) pointed out some constraints in the qualitative use of  $^{137}\text{Cs}$  time-markers. Consequently, it is advisable to interpret activity profiles of  $^{137}\text{Cs}$  and other man-made radionuclides with appropriate models. As the inputs of anthropogenic radionuclides into the sediment vary with time, steady-state cannot be assumed; thus, the mathematical advection–diffusion problem requires providing the time series of such historical inputs.

This work addresses a method for reconstructing historical records of depth-averaged  $^{137}\text{Cs}$  and  $^{239+240}\text{Pu}$  concentrations in water (and their corresponding fluxes into the sediment) in a marine environment, in combination with the radiometric dating of the sediment core, using three independent records: unsupported  $^{210}\text{Pb}$ ,  $^{137}\text{Cs}$  and  $^{239+240}\text{Pu}$ .

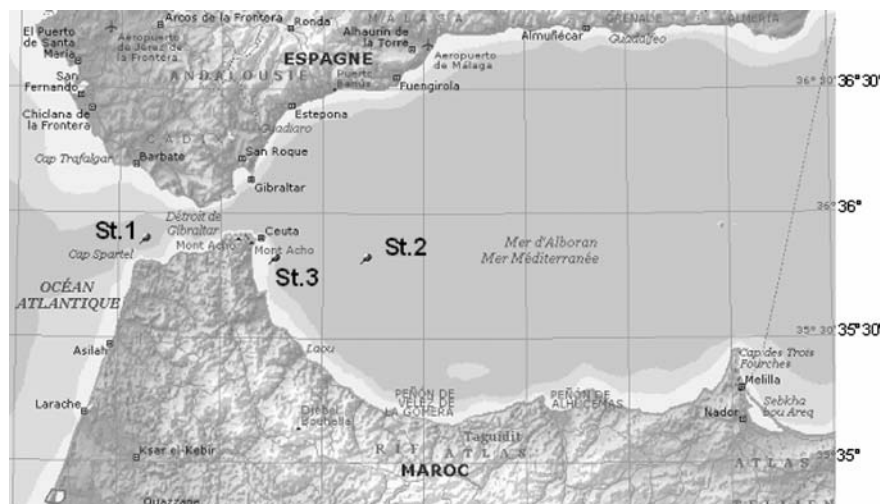
## Materials and methods

Three stations in the southwest Mediterranean Sea (the Alboran Sea and Strait of Gibraltar) were sampled. The cruise was carried out in December 1999 using the R/V Charif Al Idrissi of the Institut National de la Recherche Halieutique (INRH) (Benmansour et al. 2006). Sampling points are shown in Fig. 1. Station 2 located at  $35^{\circ}47' \text{ N}$ ,  $04^{\circ}48' \text{ W}$  was extensively explored by collecting water profile samples at different depths down to 900 m, and a bottom sediment core collected at a water depth of 800 m using a 40 cm  $\times$  40 cm box corer (Ocean Instruments).

### Seawater analysis

Due to low concentrations of transuranic elements, large volumes of water ( $\sim 200 \text{ l}$ ) were sampled using 30-l Niskin bottles. The water samples were promptly filtered through membrane filters of 0.45  $\mu\text{m}$  pore size to remove suspended matter. Appropriate tracers of  $^{242}\text{Pu}$  and  $^{243}\text{Am}$ , and a stable Cs carrier were added, after acidifying the samples with concentrated HCl to pH 1–2, to serve as indicators of chemical

**Fig. 1** Sampling stations in the southwest Alboran Sea and the Strait of Gibraltar



recoveries. Sequential separations of radionuclides were carried out on board by co-precipitating Pu and Am, along with the other actinides, using manganese dioxide ( $\text{MnO}_2$ ) (La Rosa et al. 2005).  $^{137}\text{Cs}$  was precipitated by physical adsorption onto ammonium phosphomolybdate (AMP) at pH 1–2. A known amount of AMP was added and the mixture was stirred for a period of about 30 min. After settling, the concentrate was recovered by decantation, dried, placed in a container utilizing standard geometry, and counted in a CANBERRA low background gamma spectrometer system (resolution: 2KeV and relative efficiency: 30%). For alpha-emitters such as  $^{239+240}\text{Pu}$  and  $^{241}\text{Am}$  suitable radiochemical methods were applied for their extraction from seawater (Lee et al. 2001; La Rosa et al. 2001). Briefly, Pu was separated from Am by anion-exchange resin AG1x8. Am was co-precipitated with calcium oxalate and extracted into dibutyl-*N,N*-diethylcarbamoyl phosphonate (DDCP) and finally separated from rare earths by anion exchange in mineral acids-methanol media. Both Pu and Am fractions were electrodeposited on stainless steel discs and the resulting alpha-sources were analysed by alpha-ray spectrometry using silicon surface barrier detectors (EG&G) coupled to a PC running under Maestro<sup>TM</sup> data acquisition software.

#### Sediment analysis

The core was sectioned into slices of 0.5–1 cm thickness. The sediment samples were freeze-dried,

ground to a fine powder and homogenized before radiometric analyses. Bulk densities were determined from water content of each slice. Measurement of  $^{137}\text{Cs}$  was performed through the detection of the 662 KeV photon. Determination of  $^{226}\text{Ra}$  was carried out by the detection of the 352 KeV photon emitted by  $^{214}\text{Pb}$  after sealing for a period of 21 days to allow  $^{222}\text{Rn}$  ingrowth. All gamma measurements were performed using an HPGc detector (n-type) with resolution of 2 keV and a relative efficiency of 50% at 1,332 keV.

Total  $^{210}\text{Pb}$  concentrations in sediments were inferred by measurement of the daughter product,  $^{210}\text{Po}$ , by alpha spectrometry. About 1 g of dry, homogenized sediment was weighed into an acid-cleaned Teflon beaker, spiked with  $^{209}\text{Po}$  yield tracer and totally digested using a mixture of concentrated  $\text{HNO}_3$ -HF. The acid digest was transferred to a clean beaker and treated by repeated evaporation with HCl-boric acid solution and then dissolved in 80 ml of 0.5 M HCl. Polonium was self-deposited on a Pt disc and the activity measured by alpha-spectrometry. Unsupported  $^{210}\text{Pb}$  activity was obtained by subtracting  $^{226}\text{Ra}$  activity from the total  $^{210}\text{Pb}$  activity.

$^{239+240}\text{Pu}$  was determined in aliquots of about 10 g of sediment by oxidation state adjustment using anionic exchange resin after wet leaching in  $\text{HNO}_3/\text{H}_2\text{O}_2$  dissolution.  $^{242}\text{Pu}$  was added as an internal tracer at the beginning of the radiochemical process to determine the chemical recoveries. The final solutions were electroplated onto stainless steel discs and counted as for the water samples.

## Results and discussion

### Seawater

Table 1 lists  $^{137}\text{Cs}$ ,  $^{239+240}\text{Pu}$  and  $^{241}\text{Am}$  activity concentrations in surface waters for the three stations, as well as in water profile samples collected to a depth of 900 m at Station 2, located in the southwest Alboran Sea. Some  $^{241}\text{Am}$  activity concentrations are not given due to low recoveries of the radiochemical procedures.

From recent Mediterranean studies (Molero et al. 1995; Merino et al. 1997; Sanchez Cabeza and Molero 2000; Lee et al. 2003),  $^{137}\text{Cs}$  activity concentrations in surface seawater have been between 2.3 and 5.6  $\text{mBq l}^{-1}$ , which are in close agreement with the values found in this work.  $^{137}\text{Cs}$  activity concentrations in the water profile (Fig. 2) do not show a noticeable surface maximum as the concentration at 900 m water depth is comparable with the concentration at the surface.

The  $^{239+240}\text{Pu}$  surface activity concentrations determined in this work range between 8.29 and 8.92  $\mu\text{Bq l}^{-1}$ , and they are comparable with the data reported by León Vintró et al. (1999) in the same zone 10 years earlier, as well as with recent data published by Lee et al. (2003). The vertical distribution of  $^{239+240}\text{Pu}$  in the water column of Station 2 shows a typical sub-surface maximum at a depth close to 500 m (Fig. 2). This behavior was already observed in previous studies (Fukai et al. 1979; Mitchell et al. 1995; Merino et al. 1997; León Vintró et al. 1999; Fowler et al. 2000; Lee et al. 2003). This has been usually attributed to the removal of the plutonium from the surface in association with

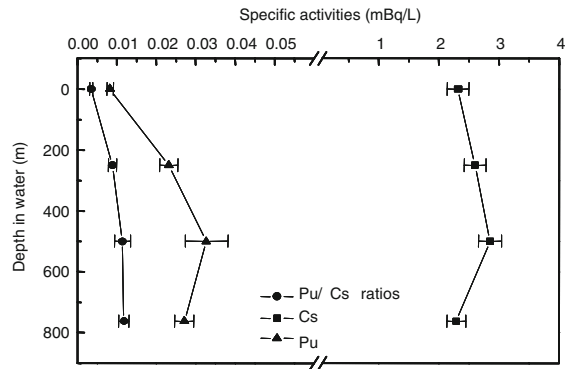


Fig. 2 Vertical distributions of  $^{137}\text{Cs}$  and  $^{239+240}\text{Pu}$  in the water column for Station 2 (from Table 1)

scavenging processes, its transport with suspended matter to deeper water layers, and the subsequent particle dissolution/remineralization at depth, with the return of plutonium into the solution.

Only a few results have been obtained for  $^{241}\text{Am}$  in this work. The mean  $^{241}\text{Am}$  activity concentration in surface water was  $1.53 \pm 0.18 \mu\text{Bq l}^{-1}$ . This value is similar to that given by Lee et al. (2003) in a recent study in the northwest Mediterranean Sea ( $\sim 1.5 \mu\text{Bq l}^{-1}$ ), and to that measured earlier by Molero et al. (1995) along the Spanish Mediterranean coast ( $\sim 1.0 \mu\text{Bq l}^{-1}$ ). The  $^{241}\text{Am}$  activity concentration at a depth of 500 m was  $7.6 \pm 1.2 \mu\text{Bq l}^{-1}$ , much higher than at the surface. Its behavior in the water column is therefore similar to Pu.

The total radionuclide inventories of  $^{137}\text{Cs}$  and  $^{239+240}\text{Pu}$  in the water column were calculated by integration of the concentration profiles, assuming a

Table 1  $^{137}\text{Cs}$ ,  $^{239+240}\text{Pu}$  and  $^{241}\text{Am}$  activity concentrations in surface seawater and in the water column

Station	$^{137}\text{Cs}$ ( $\text{mBq l}^{-1}$ )	$^{239+240}\text{Pu}$ ( $\mu\text{Bq l}^{-1}$ )	$^{241}\text{Am}$ ( $\mu\text{Bq l}^{-1}$ )	$^{241}\text{Am}/^{239+240}\text{Pu}$	$^{239+240}\text{Pu}/^{137}\text{Cs}$
St. 1 (Tangier) (35°52' N, 5°51' W)	$3.11 \pm 0.23$	$8.29 \pm 0.94$	ND	ND	$0.0027 \pm 0.0003$
St. 2 (Mdiq) (35°47' N, 4°48' W)					
0 m	$2.32 \pm 0.18$	$8.29 \pm 0.87$	$1.50 \pm 0.20$	$0.18 \pm 0.03$	$0.0035 \pm 0.0004$
250 m	$2.46 \pm 0.18$	$23.2 \pm 2.3$	ND	ND	$0.0089 \pm 0.0010$
500 m	$2.50 \pm 0.19$	$32.7 \pm 5.4$	$7.6 \pm 1.2$	$0.23 \pm 0.05$	$0.0114 \pm 0.0020$
900 m	$2.29 \pm 0.16$	$27.1 \pm 2.4$	ND	ND	$0.0118 \pm 0.0013$
St. 3 (Mdiq) (35°47' N, 5°15' W)	$2.37 \pm 0.14$	$8.82 \pm 1.39$	$1.56 \pm 0.50$	$0.17 \pm 0.02$	$0.0037 \pm 0.0006$

Reported uncertainties are  $\pm 1\sigma$ ; ND, not determined

linear variation in concentration between the sampled points. The values were found to be  $2,170 \text{ Bq m}^{-2}$  and  $23 \text{ Bq m}^{-2}$  respectively. Concordant values of  $^{137}\text{Cs}$  inventories in the west Mediterranean have been reported earlier:  $3,300 \text{ Bq m}^{-2}$  (Merino et al. 1997) for a water depth of 1,160 m;  $2,600 \text{ Bq m}^{-2}$  (Molero et al. 1995) for a water depth of 1,000 m.  $^{239+240}\text{Pu}$  inventory also showed similarities with those in the literature: Fowler et al. (2000) reported values ranging from 49 to  $58 \text{ Bq m}^{-2}$ ; and Molero et al. (1995) found values of  $23 \text{ Bq m}^{-2}$  for a water depth of 1,000 m.

The  $^{239+240}\text{Pu}/^{137}\text{Cs}$  activity ratio increases with depth from 0.0035 to 0.012, as expected (Lee et al. 2003), suggesting a depletion of plutonium at the surface layer in comparison with cesium due to Pu's preferential association with sinking particulate matter (Fowler et al. 2000; Lee et al. 2003). The  $^{241}\text{Am}/^{239+240}\text{Pu}$  activity ratio is estimated to be 0.18 at the surface and 0.23 at the 500 m water depth; however, this change is within the reported uncertainties.

### Sediment core profiles

Vertical distributions of specific activities of  $^{137}\text{Cs}$  and  $^{239+240}\text{Pu}$  in the sediment core are plotted in Fig. 3. These profiles do not show defined peaks that can be used as time markers (e.g., a peak associated with maximum atmospheric deposition of anthropogenic radionuclides from global fallout in 1963). The  $^{137}\text{Cs}$  and  $^{239+240}\text{Pu}$  activities ranged between  $1.90\text{--}6.27 \text{ Bq kg}^{-1}$  and  $0.307\text{--}0.796 \text{ Bq kg}^{-1}$ , respectively, and are similar to those reported in the literature (Delfanti

et al. 1995; Pappuci et al. 1996; León Vintró et al. 1999).

The total inventories for  $^{137}\text{Cs}$  and  $^{239+240}\text{Pu}$ , calculated by summing the product of each section's activity, sediment bulk density and its thickness, were  $284 \text{ Bq m}^{-2}$  for  $^{137}\text{Cs}$  and  $32 \text{ Bq m}^{-2}$  for  $^{239+240}\text{Pu}$ . Gascó et al. (2002) reported a value of  $163 \text{ Bq m}^{-2}$  for  $^{137}\text{Cs}$  and  $29 \text{ Bq m}^{-2}$  for  $^{239+240}\text{Pu}$  in the Spanish coastal margin of the Alboran Sea (water depth of 360 m). It may be noted that the activities and corresponding inventories of transuranic elements in sediments strongly depend on the sedimentation rate, which is itself a function of local hydrodynamic conditions.

Distribution coefficients,  $k_d$ , for  $^{137}\text{Cs}$  and  $^{239+240}\text{Pu}$  can be estimated from the specific activities in sediment (which vary with depth) and the overlying water. In this work,  $k_d$  is defined as the ratio between the specific activity in the upper sediment slice (0.5 cm thick) and the specific activity in the lower layer of the water column. This will be of use to estimate radionuclide inputs into the sediment from historical water column concentrations, assuming constant  $k_d$  values. Distribution coefficients are found to be  $1,620 \pm 160$  and  $(1.90 \pm 0.27) \times 10^4$  for  $^{137}\text{Cs}$  and  $^{239+240}\text{Pu}$  respectively, which are in good agreement with values reported in the literature (IAEA 2004).

### Dating of the sediment core

The activity profiles of  $^{210}\text{Pb}$  and  $^{226}\text{Ra}$ , listed in Table 2, were determined in the sediment core to achieve radiometric dating. The "excess" or unsupported  $^{210}\text{Pb}$  was obtained by subtracting the supported

**Fig. 3** Vertical distributions of  $^{137}\text{Cs}$  and  $^{239+240}\text{Pu}$  in the sediment core from the southwest Mediterranean Sea

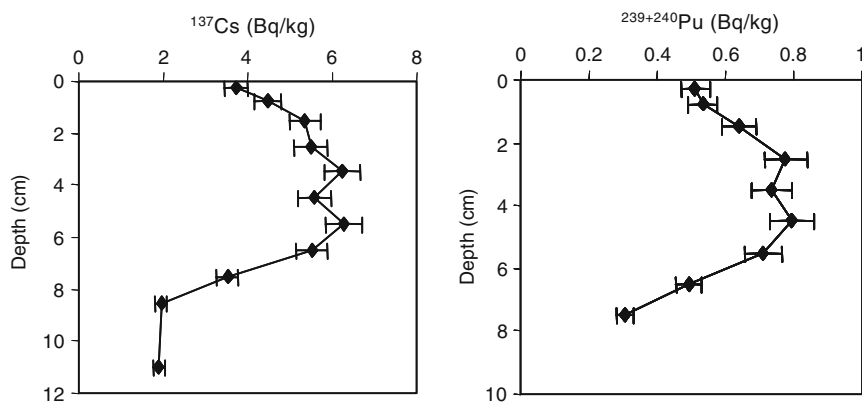


**Table 2** Vertical distribution of  $^{210}\text{Pb}$ ,  $^{226}\text{Ra}$  and bulk density in the sediment core from the southwest Mediterranean Sea sampled in December 1999 (35°47' N, 04°48' W; depth 800 m)

Depth (cm)	Bulk density ( $\text{g}/\text{cm}^3$ )	Total $^{210}\text{Pb}$ (Bq/kg)	$^{226}\text{Ra}$ (Bq/kg)	Excess $^{210}\text{Pb}$ (Bq/kg)
0–0.5	0.321	680 ± 40	28 ± 5	650 ± 40
0.5–1	0.313	690 ± 40	28 ± 5	660 ± 40
1–2	0.454	600 ± 30	25 ± 4	580 ± 30
2–3	0.645	620 ± 30	23 ± 4	600 ± 30
3–4	0.577	435 ± 16	30 ± 4	405 ± 16
4–5	0.684	316 ± 16	21 ± 3	295 ± 16
5–6	0.716	264 ± 12	24 ± 3	240 ± 12
6–7	0.697	237 ± 15	34 ± 4	203 ± 16
7–8	0.639	219 ± 11	33 ± 4	186 ± 12
8–9	0.604	210 ± 40	24 ± 3	190 ± 40
10–12	0.609	121 ± 15	28 ± 5	93 ± 16

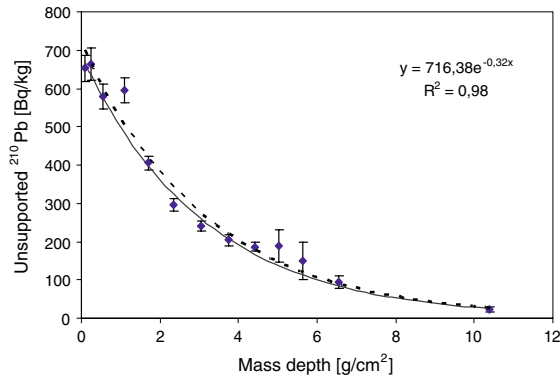


**Fig. 4** Unsupported  $^{210}\text{Pb}$  specific activity versus mass depth ( $\text{g cm}^{-2}$ ). Points are the experimental data with  $1\sigma$  errors. Dashed line is the best fit corresponding to the CIC-CSR model while the continuous line corresponds to the CM-CSR model

fraction (in secular equilibrium with  $^{226}\text{Ra}$ , with specific activities in the range 21–35  $\text{Bq kg}^{-1}$ ) from the total  $^{210}\text{Pb}$  activity. Figure 4 plots unsupported  $^{210}\text{Pb}$  specific activities versus mass thickness,  $m$  (in  $\text{g cm}^{-2}$ ). This last value is obtained from the bulk density profile,  $\rho(z)$  (given in Table 2), by the expression:

$$m(z) = \int_0^z \rho(z') dz' \quad (1)$$

Mass depth is used instead of true depth in radiometric dating models to account for compaction effects (Abril 2003a).

The CIC-CSR model assumes that initial concentration and sedimentation rate are both constant, and also assumes that there is no post-depositional mixing or diffusion. In this way, the model predicts an exponential decay for the unsupported  $^{210}\text{Pb}$  specific activity,  $A$ , versus  $m$  (shown in Fig. 4):

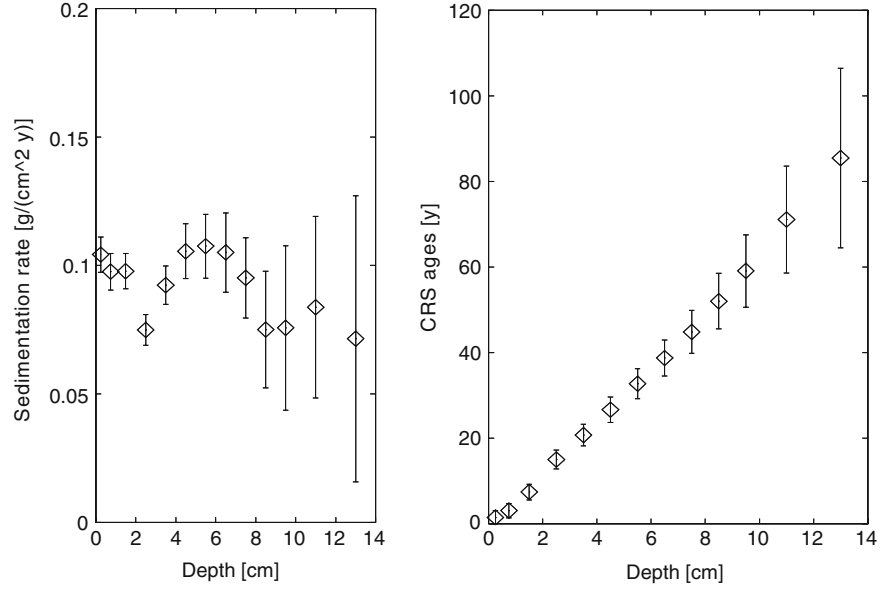
$$A(m) = A(0)\text{Exp}\left(-\frac{\lambda}{w}m\right) \quad (2)$$

where  $w$  is the sedimentation rate and  $\lambda$  the radioactive decay constant for  $^{210}\text{Pb}$ . The best fit to the data set provides for this core  $w = 0.10 \pm 0.02 \text{ g cm}^{-2} \text{ y}^{-1}$ . The annual  $^{210}\text{Pb}$  input onto the sediment,  $F$ , can be estimated from  $F = A(0)w$ , yielding a value of  $720 \pm 150 \text{ Bq m}^{-2} \text{ y}^{-1}$ .

The CRS model (Appleby and Olfield 1978) assumes a constant rate of supply of unsupported  $^{210}\text{Pb}$  and no post-depositional mixing. In this model the sediment accumulation rate can vary, (i.e., the specific  $^{210}\text{Pb}$  activity decreases when the sedimentation rate increases). This model is widely known and applied; and updated presentations can be found in Appleby (1998) and Appleby (2001). The total  $^{210}\text{Pb}$  inventory,  $\Sigma$ , is required for the CRS model. It can be obtained from Fig. 4, including a small correction for incompleteness of the profile (3.6% correction, estimated by extrapolation of an exponential fit of the lower portion of the profile), producing a value of  $22.9 \text{ kBq m}^{-2}$ . Results for sedimentation rates and ages are shown in Fig. 5. Sedimentation rates in the last 50 years are relatively uniform, with a mean value of  $0.10 \text{ g cm}^{-2} \text{ y}^{-1}$  (despite a short deceleration around 1985). The annual  $^{210}\text{Pb}$  input onto the sediment can be estimated from  $F = \lambda\Sigma$ , yielding  $712 \pm 25 \text{ Bq m}^{-2} \text{ y}^{-1}$ , in agreement (within  $1\sigma$ ) with CIC-CSR results.

A  $^{210}\text{Pb}$  geochronology should be validated using at least one independent tracer that identifies an independent, unambiguous time-stratigraphic horizon (Smith 2001; Abril 2003b, 2004). The  $^{137}\text{Cs}$  profile (Fig. 3) can be used for this purpose. The quality of data, however, precludes identification of the expected time markers corresponding to the years 1963 (maximum in  $^{137}\text{Cs}$  fallout) and 1986 (Chernobyl accident). On the other hand,  $^{137}\text{Cs}$  was measured at 11 cm depth, and if no mixing occurred, that depth should correspond to the early 1950s or later. CRS  $^{210}\text{Pb}$  dates (Fig. 5) clearly are at odds with the presence of  $^{137}\text{Cs}$  in deep horizons. Downward diffusion of  $^{137}\text{Cs}$  could explain this last point, but

**Fig. 5** Calculated CRS sedimentation rates (left) and ages (right) versus depth for the sediment core



diffusion associated with solids violates the basic assumptions of CRS and CIC-CSR models (Abril 2003b, 2004). Consequently a different model approach is required.

The unsupported <sup>210</sup>Pb profile (Fig. 4) can be explained alternatively in terms of a Constant Mixing with Constant Sedimentation Rate (CM-CSR) model:

$$A(m) = \frac{F}{w - k_m x_-} \text{Exp}(x_- m); \quad (3)$$

$$x_- = \frac{w - \sqrt{w^2 + 4\lambda k_m}}{2k_m}; \quad k_m = D\rho^2$$

where  $k_m$  is an effective mixing coefficient given in terms of the diffusion coefficient  $D$  and the bulk density (Abril 2003b). A similar model was applied by Smith et al. (1986) to Northeast Atlantic sediments. The model fit experimental data (shown in Fig. 4) and provides parameter values of  $w = 0.092 \pm 0.003 \text{ g cm}^{-2} \text{ y}^{-1}$ ,  $k_m = 0.015 \pm 0.009 \text{ g}^2 \text{ cm}^{-4} \text{ y}^{-1}$  ( $D = 0.035 \text{ cm}^2 \text{ y}^{-1}$  for deeper layers) and  $F = 670 \pm 12 \text{ Bq m}^{-2} \text{ y}^{-1}$ .

To validate the new model approach with <sup>137</sup>Cs and <sup>239+240</sup>Pu profiles it is necessary to solve the advection–diffusion equation for a particle-bound tracer in sediments under steady state compaction, and time-dependent inputs of radionuclides (Abril 2003a, b):

$$\frac{\partial A}{\partial t} = -\lambda A + \frac{\partial}{\partial m} \left( k_m \frac{\partial A}{\partial m} \right) - \frac{\partial}{\partial m} (wA) \quad (4)$$

with boundary conditions

$$F(t) = -k_m \frac{\partial A}{\partial m} \Big|_{m=0} + wA(0, t) \quad (5)$$

$$A(m \rightarrow \infty) = 0$$

This equation can be solved numerically (Abril 2003b), but the key point is  $F(t)$ , that is, the historical records of radionuclide fluxes into the sediment. If historical records of radionuclide concentration in overlying water,  $C_w$ , were available, radionuclide inputs could be estimated from sedimentation rates and  $k_d$  values:

$$F dt = k_d w C_w dt. \quad (6)$$

Unfortunately, historical data on  $C_w$  are not available. A proper reconstruction might be possible from 3D water circulation models with an appropriate description of suspended particle dynamics, and physical–chemical (and biological) transfers. This is beyond the scope of the present work. Here we will try to explain basic aspects of the measured profiles in the sediment core by using a crude approach consisting of a water column model that receives atmospheric fallout,  $F_{at}(t)$ , and has two sinks: the transfer of radionuclides to the sediment and the net losses associated with horizontal transport. As the observed depth distributions (Table 1) are quite uniform for <sup>137</sup>Cs, and the concentration of <sup>239+240</sup>Pu in deep water is close to the depth-averaged one, the model can operate with depth-averaged concentrations,  $\bar{C}_w$ . The measured  $k_d$  values reported in this work (from sediments) will be used along with the first estimate of

$w = 0.10 \text{ g cm}^{-2} \text{ y}^{-1}$  as a reasonable approach. The whole process could be iterated. Finally, the net losses due to horizontal transport will be assumed to be proportional to the water column inventory, with a proportionality factor  $k_h$ . Thus, for a water column of height  $h$  and unit cross-sectional area,

$$\frac{d\bar{C}_w}{dt} = -k_d w \bar{C}_w - k_h \bar{C}_w + Z \frac{1}{h} \frac{dF_{at}}{dt} \quad (7)$$

Time series of atmospheric fallout of  $^{137}\text{Cs}$  and  $^{239+240}\text{Pu}$  measured in Denmark by the Risø National Laboratory will be used to estimate the atmospheric deposition for the study area. Differences by latitude and other local factors can be treated as a global multiplicative constant (Abril 2003b, 2004) included in the normalization factor  $Z$ , (given by the ratio between the measured inventory in the sediment and the computed integrated fluxes of radionuclides onto the sediment). The eventual contribution from Chernobyl was very limited in this area and there is a scarcity of suitable data, consequently, it has not been explicitly included in the atmospheric inputs. Finally, the parameter  $k_h$  was selected in such a way that calculated concentrations for 1999 adequately match the measured ones (Table 1). Results are shown in Fig. 6. We note how calculated  $^{137}\text{Cs}$  concentrations in the late 1970s are in good agreement with the ones reported for the Mediterranean

Sea before the Chernobyl accident (average value of  $3.4 \text{ mBq l}^{-1}$ , range  $3.2\text{--}4.8 \text{ mBq l}^{-1}$ , from Fukai et al. 1980).

Model parameters for  $^{137}\text{Cs}$  were  $Z = 3.7$  and  $k_h = 0.036 \text{ y}^{-1}$ , while for  $^{239+240}\text{Pu}$ , the corresponding values were  $Z = 2.0$  and  $k_h = 0.0075 \text{ y}^{-1}$ . Let us discuss the physical meaning of  $Z$ . The sediment core was sampled from a deep basin, where vertical mixing causes a dilution in concentration that tends to be compensated for by horizontal mixing from the surrounding areas. Horizontal transport seems to be less efficient for highly particle-reactive radionuclides such as  $^{239+240}\text{Pu}$ . A similar situation is found for  $^{210}\text{Pb}$ . Effectively, inputs onto the sediment (some  $700 \text{ Bq m}^{-2} \text{ y}^{-1}$ ) resulted in higher values (by a factor of about 2) than those expected by direct atmospheric deposition (if compared with the estimated atmospheric deposition over Central Europe of  $55\text{--}70 \text{ R}/100 \text{ Bq m}^{-2} \text{ y}^{-1}$ , where  $R$  is the mean annual rainfall, in  $\text{mm y}^{-1}$ ; from Appleby 1998). When external inputs vanish, concentrations in waters tend to decrease following the general dynamics of water masses and the transfer to sediments and other sinks. Again, net losses due to horizontal transport (measured through parameter  $k_h$  in the model) are less efficient for  $^{239+240}\text{Pu}$ .

Equation 4 can be numerically solved using a finite differences scheme, with boundary conditions given by

**Fig. 6** Calculated (from Eq. 7) historical  $^{137}\text{Cs}$  and  $^{239+240}\text{Pu}$  (depth averaged) concentrations ( $\text{mBq l}^{-1}$ ) in the water column in the studied area

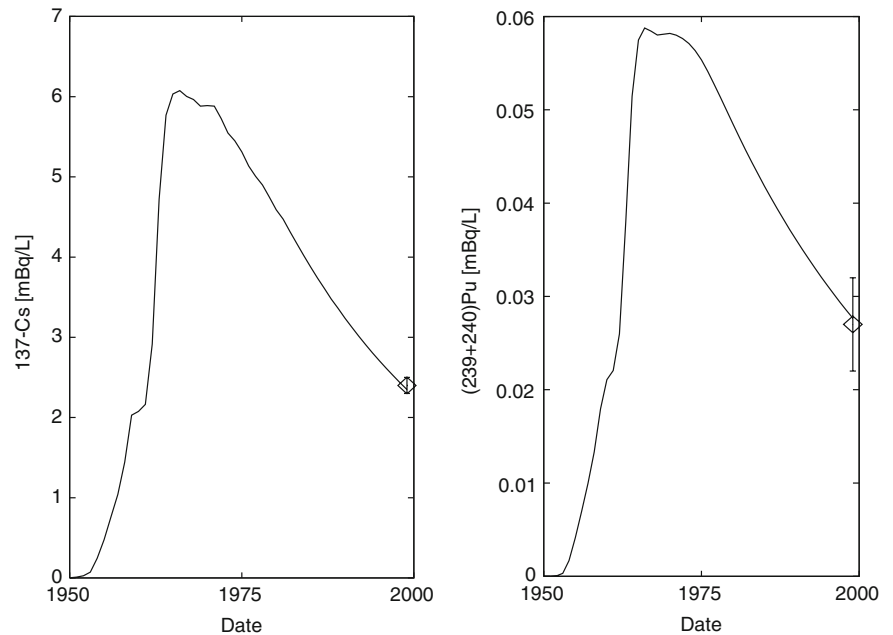
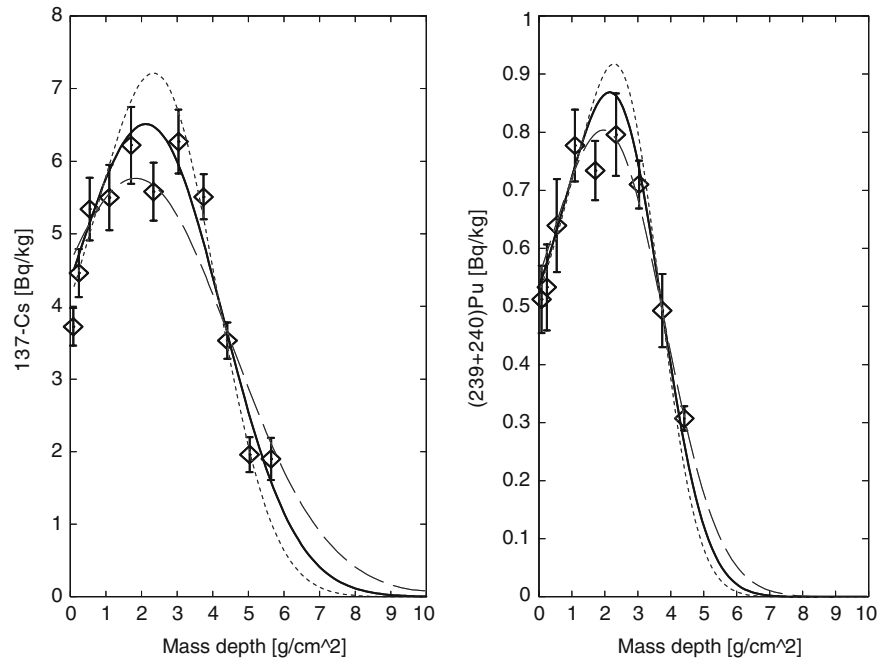




**Fig. 7** Calculated versus measured  $^{137}\text{Cs}$  and  $^{239+240}\text{Pu}$  specific activities versus mass depth profiles (continuous line). Equation 4 was solved by finite differences (upstream scheme) with  $dm = 0.01 \text{ g cm}^{-2}$  and  $dt = 0.001 \text{ y}$ . Sensitivity test for  $k_m$  is also depicted, using values of  $2k_m$  (dashed lines) and  $0.5k_m$  (dotted lines)



Eq. 5, where  $F(t)$ , the radionuclide inputs are estimated (using Eq. 6) from historical records of depth-averaged concentrations (Fig. 6). Results are shown in Fig. 7, including sensitivity tests for parameter  $k_m$ .

Model parameters for  $^{137}\text{Cs}$  were  $w = 0.10 \text{ g cm}^{-2} \text{ y}^{-1}$  and  $k_m = 0.040 \text{ g}^2 \text{ cm}^{-4} \text{ y}^{-1}$ , while for  $^{239+240}\text{Pu}$ , the corresponding values were  $w = 0.095 \text{ g cm}^{-2} \text{ y}^{-1}$  and  $k_m = 0.015 \text{ g}^2 \text{ cm}^{-4} \text{ y}^{-1}$  (values for mixing coefficients include corrections by numerical dispersion). Despite the crude approach applied to estimate historical time series of radionuclide concentrations in water and their fluxes onto the sediment, the CM-CSR model provides a reasonable interpretation of the whole data set ( $^{137}\text{Cs}$ ,  $^{239+240}\text{Pu}$  and unsupported  $^{210}\text{Pb}$  profiles). The derived sedimentation rates and mixing rates from unsupported  $^{210}\text{Pb}$  and  $^{239+240}\text{Pu}$  are in very good agreement, while the sedimentation rate derived from  $^{137}\text{Cs}$  was slightly higher, although reasonable, taking into account the model assumptions. The mixing coefficient is also higher for  $^{137}\text{Cs}$ , as expected, due to its lower  $k_d$  value, and thus more efficient mixing through desorption/adsorption processes and transport through the pore water.

Some further refinement is possible by recalculating Eqs. 6 and 7 with the final value of  $w = 0.092 \text{ g cm}^{-2} \text{ y}^{-1}$  (from the unsupported  $^{210}\text{Pb}$

profile by applying the CM-CSR model), but the present approach is enough to show global consistency of the model. From the global consistency of the data, it can be concluded that the contribution from Chernobyl was not significant in this area. Thus, no direct contribution (through  $F_{at}$ ) needs to be included in the water-column model and that is consistent with the fact that Chernobyl affected mainly the eastern and northern parts of the Mediterranean Sea. On the other hand, the term accounting for net losses by horizontal transport does not need any correction due to the intrusion of more contaminated waters coming from the western Mediterranean basin. This result is consistent with the known dynamics of the water masses. It is well known from physical oceanography that the Mediterranean Sea has two main basins, separated by the Sicilian border, with little exchange of water masses among them and that the Mediterranean outflow waters originate mainly in the western basin.

## Conclusions

- The mean activity concentrations in surface seawater in the studied area of the Alboran Sea ( $35^\circ 47' \text{ N}$ ,  $04^\circ 48' \text{ W}$ ) were around  $2.7 \text{ mBq l}^{-1}$ ,  $8.7 \text{ } \mu\text{Bq l}^{-1}$  and  $1.5 \text{ } \mu\text{Bq l}^{-1}$  for  $^{137}\text{Cs}$ ,  $^{239+240}\text{Pu}$

and  $^{241}\text{Am}$ , respectively. These values are in agreement with those reported in recent studies carried out in the western Mediterranean Sea, and are within the ranges of concentrations expected from global fallout.

- The vertical distributions of  $^{239+240}\text{Pu}$  in the water column showed a sub-surface maximum at 500 m water depth, while  $^{137}\text{Cs}$  concentrations were constant up to 900 m. The total inventories of  $^{137}\text{Cs}$  and  $^{239+240}\text{Pu}$  in the water column (0–900 m) were estimated to be 2,170 and 23  $\text{Bq m}^{-2}$ , respectively, within the expected values for these waters and depths.
- A simple 3-parameter water-column model was applied using atmospheric fallout data from Risø National Laboratory, and a first estimate of sedimentation rates—from a CRS  $^{210}\text{Pb}$  dating model and calibrated from measured data ( $k_d$  values, inventories and actual concentrations in seawater). It provided the basic features for the reconstruction of historical records of depth-averaged  $^{137}\text{Cs}$  and  $^{239+240}\text{Pu}$  concentrations in water, and their corresponding fluxes into the sediment.
- These records provided the required boundary conditions for a CM-CSR radiometric dating model that could explain quantitatively the three independent records (unsupported  $^{210}\text{Pb}$ ,  $^{137}\text{Cs}$  and  $^{239+240}\text{Pu}$  specific activities versus mass depth profiles), with a sedimentation rate of  $0.092 \pm 0.03 \text{ g cm}^{-2} \text{ y}^{-1}$ .
- The results of this exercise show that both direct and delayed contributions of radionuclides from the Chernobyl accident were negligible in this area, and that the combined effect of vertical and horizontal mixing resulted in focusing of atmospheric inputs. After the 1963-related maximum in water concentrations, the dominant effect was progressive dilution by transfer onto sediment and by horizontal circulation, the latter process being greater for  $^{137}\text{Cs}$  than for the highly particle-reactive  $^{239+240}\text{Pu}$ .

**Acknowledgements** This work was supported by IAEA under the Regional Project RAF/7/004. The authors acknowledge the support provided by IAEA-Marine Environment Laboratory of Monaco for the sampling cruise. They also thank colleagues from INRH for their assistance during sampling.

## References

- Abril JM (2003a) A new theoretical treatment of compaction and the advective–diffusive processes in sediments: a reviewed basis for radiometric dating models. *J Paleolimnol* 30:363–370
- Abril JM (2003b) Difficulties in interpreting fast mixing in the radiometric dating of sediments using  $^{210}\text{Pb}$  and  $^{137}\text{Cs}$ . *J Paleolimnol* 30:407–414
- Abril JM (2004) Constraints on the use of  $^{137}\text{Cs}$  as a time-marker to support CRS and SIT chronologies. *Environ Pollut* 129:31–37
- Abril JM, García-León M, García-Tenorio R, Sánchez CI, El-Daoushy F (1992) Dating of marine sediments by an incomplete mixing model. *J Environ Radioact* 15: 135–151
- Appleby PG (1998) Dating recent sediments by  $^{210}\text{Pb}$ : problems and solutions. In: Ilus E (ed) *Dating of sediments and determination of sedimentation rate. Proceedings of a seminar held in Helsinki Stuk A145:7–24*
- Appleby PG (2001) Chronostratigraphic techniques in recent sediments. In: Last WL, Smol JP (eds) *Tracking environmental change using lake sediments, vol 1. Basin analysis, coring, and chronological techniques*. Kluwer Academic Publishers, Dordrecht, pp 171–203
- Appleby PG, Olfield F (1978) The calculation of lead-210 dates assuming a constant rate of supply of unsupported  $^{210}\text{Pb}$  to the sediment. *Catena* 5:1–8
- Benmansour M, Laissaoui A, Benbrahim S, Ibn Majah M, Chafik A, Povinec P (2006) Distribution of anthropogenic radionuclides in Moroccan coastal waters and sediments. *Radioact Environ* 8:148–155
- Delfanti R, Desideri D, Martinotti W, Assunta Melti M, Pappucci C, Queiraza G, Testa C, Triulzi C (1995) Plutonium concentration in sediment cores collected in the Mediterranean Sea. *Sci Total Environ* 173/174:187–193
- Fowler SW, Noshkin VE, La Rosa J, Gastaud J (2000) Temporal variations in plutonium and americium inventories and their relation to vertical transport in the northwest Mediterranean Sea. *Limnol Oceanogr* 45:446–458
- Fukai R, Holm E, Ballestra S (1979) A note on vertical distribution of plutonium and americium in the Mediterranean Sea. *Oceanologica Acta* 2:129–132
- Fukai R, Ballestra S, Vas D (1980) Distribution of  $^{137}\text{Cs}$  in the Mediterranean Sea. In: *Management of environment*, Wiley Eastern Ltd, New Delhi, pp 353–360
- Gascó C, Antón MP, Pozuelo M, Meral J, González AM, Pappucci C, Delfanti R (2002) Distribution of Pu, Am and Cs in margin sediments from the western Mediterranean (Spanish coast). *J Environ Radioact* 59:75–89
- Holm E, Fukai R, Whitehead NE (1988) Radiocesium and transuranium elements in the Mediterranean Sea: sources, inventories and environmental levels. In: *International Conference on environmental radioactivity in the Mediterranean Area*. SNE. Barcelona, pp 601–617
- IAEA (International Atomic Energy Agency) (2004) *Sediment distribution coefficients and concentration factors for biota in the marine environment*. Technical Report Series 422, Vienna, ISBN 92-0-114403-2

- Laissaoui A, Abril JM (1999) A theoretical technique to predict the distribution of radionuclides bound to particles in surface bottom sediments. *J Environ Radioact* 44:71–84
- Laissaoui A, Abril JM, Perriñez R, García-León M, García-Montano E (1998) Determining kinetic transfer coefficients for radionuclides in estuarine waters: reference values from Ba-133. *J Radioanal Nucl Chem* 237(1–2): 55–61
- La Rosa J, Burnett W, Lee SH, Levy I, Gastaud J, Povinec PP (2001) Separation of actinides, caesium and strontium from marine samples using extraction chromatography and adsorbents. *J Radioanal Nucl Chem* 248:765–770
- La Rosa J, Gastaud J, Lagan L, Lee SH, Levy-Palomo I, Povinec PP, Wyse E (2005) Recent developments in the analysis of transuranics (Np, Pu, Am) in seawater. *J Radioanal Nucl Chem* 263(2):427–436
- Lee SH, Gastaud J, La Rosa J, Liang Wee Kwong L, Povinec PP, Wyse E, Fifield LK, Hausladen PA, Di Tada LM, Santos GM (2001) Analysis of plutonium isotopes in marine samples by radiometrics, ICPMS and AMS techniques. *J Radioanal Nucl Chem* 248:754–764
- Lee SH, La Rosa J, Levy-Palomo I, Oregioni B, Pham MK, Povinec PP, Wyse E (2003) Recent inputs and budgets of  $^{90}\text{Sr}$ ,  $^{137}\text{Cs}$ ,  $^{239,240}\text{Pu}$  and  $^{241}\text{Am}$  in the northwest Mediterranean Sea. *Deep-Sea Res II* 50:2817–2834
- León Vintró I, Mitchell PI, Condren OM, Downes AB, Papucci C, Delfanti R (1999) Vertical and horizontal fluxes of plutonium and americium in the western Mediterranean and the strait of Gibraltar. *Sci Total Environ* 237/238: 77–91
- Merino J, Sánchez-Cabeza JA, Bruach JM, Masqué P, Pujol LI (1997) Artificial radionuclides in high resolution water column profile from the Catalan Sea (the Northwestern Mediterranean). *Radioprotection – Colloques* 32: C285–C290
- Mitchell PI, Vives J, Batlle I, Downes AB, Condren OM, León Vintró L, Sánchez-Cabeza JA (1995) Recent observations on the physico-chemical speciation of plutonium in the Irish Sea and the Western Mediterranean. *Appl Radiat Isot* 46:1190–1995
- Molero J, Sanchez-Cabeza JA, Merino J, Pujol LI, Mitchell PI, Vial-Quadras A (1995) Vertical distribution of radiocesium, plutonium and americium in the Catalan Sea (Norwest Mediterranean). *J Environ Radioact* 26:205–216
- Papucci C, Charmasson S, Delfanti R, Gasco C, Mitchell P, Sanchez-Cabeza JA (1996) Time evolution and levels of man-made radioactivity in the Mediterranean Sea, In: Guéguéniat P, Germain P, Métivier H (eds) *Radionuclides in the oceans: input and inventories*. Les éditions de physique, pp 177–197
- Robbins JA (1978) Geochemical and geophysical applications of radioactive lead isotopes. In: Nriago JP (ed) *Biochemistry of lead in the environment*. Elsevier, Amsterdam, pp 285–393
- Robbins JA, Edgington DN (1975) Determination of recent sedimentation rates in Lake Michigan using  $^{210}\text{Pb}$  and  $^{137}\text{Cs}$ . *Geochim Cosmochim Acta* 39:285–304
- Sánchez-Cabeza JA, Molero J (2000) Plutonium, americium and radiocesium in the marine environment close to the Vandellos I nuclear power plant before decommissioning. *J Environ Radioact* 51:211–228
- Smith JN (2001) Why should we believe  $^{210}\text{Pb}$  sediment geochronologies? *J Environ Radioact* 55:121–123
- Smith JN, Boudreau BP, Noshkin V (1986) Plutonium and  $^{210}\text{Pb}$  distributions in Northeast Atlantic sediments: sub-surface anomalies caused by non-local mixing. *Earth Planet Sci Lett* 81:15–28
- UNEP, United Nations Environmental Programme (1992) Assessment of the state of pollution of the Mediterranean Sea by radioactive substances. MAP Technical Reports Series 62, Athens 60